Article:
Kamil, SA, Chandrappan, J, Murray, M et al. (3 more authors) (2016) Ultrafast laser plasma doping of Er3+ ions in silica-on-silicon for optical waveguiding applications. Optics Letters, 41 (20). pp. 4684-4687. ISSN 0146-9592

https://doi.org/10.1364/OL.41.004684

Ultrafast laser plasma doping of Er^{3+} ions in silica-on-silicon for optical waveguiding applications

Suraya Ahmad Kamil,[1] Jayakrishnan Chandrappan,[1,*] Matthew Murray,[1] Paul Steenson,[2] Thomas F. Krauss,[3] Gin Jose[1]

[1]*Applied Photon Science, School of Chemical and Process Engineering, University of Leeds, Leeds, LS2 9JT, UK*
[2]*Institute of Microwave and Photonics, School of Electronics and Electrical Engineering, University of Leeds, Leeds, LS2 9JT, UK*
[3]*Department of Physics, University of York, York, YO10 5DD, UK*
**Corresponding author: J.Chandrappan@leeds.ac.uk*

Received XX Month XXXX; revised XX Month, XXXX; accepted XX Month XXXX; posted XX Month XXXX (Doc. ID XXXXX); published XX Month XXXX

An ultrafast laser plasma doping (ULPD) technique is used to high concentration doping of erbium ions into silica-on-silicon substrate. The method uses femtosecond laser to ablate material from TeO_2-ZnO-Na_2O-Er_2O_3 (Er-TZN) target glass. The generated plasma modifies the silica network, producing high index contrast optical layer suited to the production of on-chip integrated optical circuits. Cross-sectional analysis using scanning electron microscope with energy dispersive x-ray spectroscopy revealed homogenous intermixing of the host silica with Er-TZN, which is unique to ULPD. The highly doped layer exhibits spectroscopic characteristics of erbium with photoluminescence lifetimes ranging from 10.79 ms to 14.07 ms.

Silica-on-silicon (SOS) integrated optical waveguides are widely used in applications such as arrayed waveguide gratings [1], optical switches [2] and quantum optical circuits [3]. Such integrated optical circuits (IOC) are mandatory to support the year-on-year growth of internet traffic, to name but one application. A typical IOC involves the dense integration of optical components such as; lasers, modulators, waveguide arrays, splitters, filters and photodetectors [4]. Inherent losses suffered by the optical signals in such dense integration would ideally be compensated for by an on-chip optical amplifier. The erbium doped waveguide amplifier (EDWA) is considered as an ideal candidate to fulfil this need, due to its compatibility with CMOS fabrication technology [5], its high gain and low noise in the C-band of optical communication [6].

The choice of host material for an EDWA significantly impacts the achievable gain per unit length, as it is closely linked to the material characteristics, such as erbium (Er^{3+}) concentration solubility and photoluminescence (PL) lifetime [7]. Identifying a suitable host which enables an enhancement of all of these useful characteristics and which is beyond current EDWA capabilities, would enable such a material to become the *de facto* standard for IOC realization. Tellurites offer a higher solubility for erbium and tellurite based waveguides have been shown to produce internal gain as high as 2.8 dB/cm [8]. A few erbium doped tellurite based glasses, such as TeO_2-WO_3-Na_2O-Er_2O_3 [9] and TeO_2-GeO_2-Na_2O-ZnO-Er_2O_3 [10] have been successfully fabricated as waveguides. However, tellurite glasses do have serious drawbacks because of their relatively low thermal stability. This attribute renders such materials unsuitable for practical applications [11]. Silica is the obvious candidate due to its refractive index matching to that of silica optical fibers, thus minimizing coupling losses. A key limitation with silica is its limited solubility for erbium, and even moderate concentrations (0.7×10^{18} cm^{-3}) of Er^{3+} ions tend to induce clustering [12]. This low solubility limit is partly due to the continuous network of tetrahedral units in silica, which do not accommodate Er^{3+} ions effectively [13]. Er^{3+} ions have a preference to achieve a larger coordination number, typically six. Hence, Er^{3+} ions are likely to position themselves close to each other (cluster) to facilitate this and achieve their preferred six-fold coordination [14]. Upon clustering, the Er-Er energy transfer process tends to result in quenching of the luminescence through non-radiative relaxation of the ion pair, which manifests itself in a reduced PL lifetime of the metastable $^4I_{13/2}$ state [15]. Typically, a concentration of 10^{20}-10^{21} Er^{3+} ions/cm^3 is required without concentration quenching and shortening of the metastable lifetime in order to achieve a reasonable gain over a length of a few centimeters [16].

The solubility of erbium in pure silica (SiO_2) can be increased by adding other oxide materials to the glass composition such as P_2O_5 [17] and Al_2O_3 [18]. The addition of such materials increases the non-bridging oxygen (NBO) sites in the SiO_2 glass to which the Er^{3+} ions bond and neutralize their positive charges. This in turn increases the NBO sites, raising the overall solubility limit of silica. However, competition among Er^{3+} ions to gain oxygen atoms still results in clustering at higher concentrations [13]. Er^{3+} ions doped into other Si-based host materials such as silica-hafnia (SiO_2-HfO_2) [19], SiO_2-Ta_2O_5 [20], and aluminophosphosilicate [21] glasses have also been demonstrated, but only with limited success.

Regarding other fabrication methods, such as; RF sputtering [22], sol-gel glass deposition [19,20], plasma enhanced chemical vapor deposition (PECVD) [23] and flame hydrolysis deposition (FHD) [24], these have all been tried, but none have so far been

sufficiently successful to be applied for practical optical amplifier devices. For example, the sol-gel approach [25] resulted in cracked thin-films caused by shrinkage during annealing. FHD has been limited to a doping density of 0.45 wt% (~$4x10^{19}$ cm^{-3}) [16,24], in the core layer, due to clustering which is associated with the high temperature (around 1300 °C) typically used in this technology [26]. For PECVD, it is the low vapor pressure of erbium compound which makes it difficult to achieve sufficiently high concentrations. Consequently, the internal gain achieved via PECVD is only 0.35 dB/cm [21,27]. As for sputtering, the film surface tends to be rough and porous, which increases scattering losses [22].

Consequently, all the above methods failed to sufficiently improve the doping concentration of Er^{3+} ions in silica. The work presented here shows that these limitations can be overcome by the ultrafast laser plasma doping (ULPD) technique which we have recently optimized. This technique allowed the doping of silica with record high concentrations of rare-earth (Er/Yb) elements. In our studies, TeO_2-ZnO-Na_2O-Er_2O_3 (Er-TZN) glass targets, prepared by a standard glass melt quenching process, were ablated using a femtosecond (fs) laser (100 fs-pulsed, wavelength of 800 nm) forming complex layers on various substrates. The interfacial reactions between the high energy plasma and the hot silica glass substrates produced highly dense Er-doped silicates which we refer to as erbium-doped tellurite modified silica (EDTS). An erbium concentration as high as 0.91 x 10^{21} atoms/cm^3 with an accompanying lifetime of 10.56 ms and 1.63 x10^{21} atoms/cm^3 with a lifetime of 9.1 ms for Er^{3+}/Yb^{3+}, and without any detectable clustering, was achieved in this research [28,29]. This is approximately an order of magnitude higher than the concentrations reported by any other methods.

We now report the application of this approach to form active planar waveguides on SOS substrates. The use of Er-TZN target materials affords a high erbium concentration for the ULPD process as tellurite based glass has high solubility of erbium [30]. Additionally, the heavy elements such as Te and Er increased the refractive index of the doped layer, which is especially convenient for realizing good optical waveguides. The high index contrast between the waveguide core and the cladding can be controlled making it suitable for single mode operation at the optical communication wavelength of 1550 nm. ULPD could therefore uniquely facilitate the fabrication of integrated optical circuits on SOS.

To ablate the target, the fs-laser was focused onto the surface at an angle of incidence of 60°. The target was then rastered within a vacuum chamber and allowing it to be both rotated and rastered at the same time, ensuring uniform wear of the target and good uniformity in the layers so formed as a result of the stable and consistent plasma plume. Commercially available SOS (IDB technologies) was used as a substrate with the silica layer of thickness 1 µm grown by thermal oxidation. The cleaned SOS substrate was positioned 70 mm above the target with the silica surface facing the target. Subsequently, the chamber was pumped down to below 8 x 10^{-6} mTorr before backfilling with oxygen to give a background pressure of 70 mTorr. The substrate was heated to 570 °C and then exposed to the plasma plume resulting from the femtosecond laser ablation for 4 hours to obtain the multi-ion doped samples.

Samples prepared by ULPD were analyzed using a Hitachi SU8230 scanning electron microscope (SEM) and energy dispersive X-ray (EDX). The cross-section image allowed clear identification of the EDTS layer thickness (Fig. 1), which was confirmed using a Metricon 2010 prism coupler. EDX was used to determine the elemental composition of the EDTS layers. The refractive index of the doped layers were determined by the prism coupling technique. X-ray diffraction (XRD) using a Philips X'Pert was employed to detect the presence of any crystalline phases in the doped layers. Samples were scanned using Cu K_α radiation from 10° to 85° with a step size of 0.05 °/s at room temperature in air. The PL emission spectra were also examined with an Edinburgh Instruments FLS920 spectrometer using a 980 nm laser excitation and the lifetimes were also studied using time-resolved PL spectra, whereby the laser source was pulsed using a 100 ms period and a pulse width of 10 µs.

Figure 1(a) shows backscattered cross-section SEM images of the bare SOS substrate. Figures 1(b)-1(d) show the cross-sections of the samples prepared with different laser energies. The contrast differences seen within each micrograph gives some comparative indication of the density of the different layers. Sample A1 (Fig. 1(b)), A2 (Fig. 1(c)) and A3 (Fig. 1(d)) represent samples prepared using fs-laser energies of 50, 60 and 80 µJ, respectively while all other parameters were kept identical. The elemental composition of the EDTS layers obtained are presented in Table 1, confirms the presence of the various cations removed from the target glass.

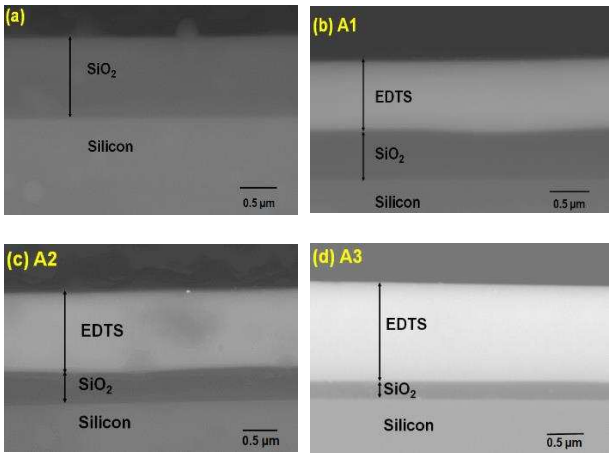

Fig. 1. Backscattered SEM cross section images of (a) bare silica-on-silicon substrate, then Er-TZN doped into silica-on-silicon substrate using fs-laser energy at; (b) 50 µJ (A1) (c) 60 µJ (A2), and (d) 80 µJ (A3)

In these SEM images, the EDTS layer always looks brighter than the silicon and silica layers. Which, as mentioned earlier is due to the presence of heavy elements such as Te and Er in EDTS, which naturally results in a stronger average backscattered electron flux. By comparison, the silica layer is rich with lighter elements such as oxygen, which caused the layer to look darker. The samples did not show any detectable clustering of Er^{3+} ions. The dynamics of the layer formation process is that the high energy laser-plasma plume strikes the already hot substrate material and it is the heating of the substrate which provides the activation energy needed to mediate this process and dynamically brake and remake the strong Si-O-Si-covalent bonds in the silica. This helps the high energy ions from the target glass penetrate into the silica and modify the host glass

network [28,29]. As a result, a well-defined metastable homogenous EDTS layer is produced. It was observed by EDX (Table 1), that the concentration of Te, Zn, Na and Er is increased in EDTS when a higher laser energy is used, which is consistent with the increased volume of target material removed during the ablation process. This would also explain the increased of EDTS refractive index (Table 2) as measured by the prism coupler method as more elements from the target material i.e. the heavy elements such as Te and Er integrated in EDTS when higher laser energy was used. Furthermore, the doped layers were also found to be thicker with increased laser energy from the SEM images and prism coupler measurements (Table 2) and this is to be expected given a higher incident ion flux. The pristine silica layer thickness is reduced due to the modification of silica surface by the transformation into EDTS, and especially so, with increased laser energy. This volume expansion of the EDTS was not obvious in our previous research which was based on bulk silica glass substrates [28,29]. By increasing the laser energy, the EDTS layer eventually cracked or ruptured for energies of 100 µJ due to the high surface strain. As the 100 µJ sample was considered damaged, we did not perform any characterization on this sample.

Table 1: Elemental composition of EDTS layer for different laser energy measured by EDX in atomic percent (at. %). The estimated uncertainty is ± 0.01 at.%.

Element	Laser energy of 50 µJ (A1)	Laser energy of 60 µJ (A2)	Laser energy of 80 µJ (A3)
O	66.76 at.%	64.20 at.%	57.89 at.%
Na	3.29 at.%	4.94 at.%	12.08 at.%
Si	21.32 at.%	21.06 at.%	17.82 at.%
Zn	6.97 at.%	7.36 at.%	7.54 at.%
Te	1.06 at.%	2.00 at.%	4.14 at.%
Er	0.40 at.%	0.43 at.%	0.53 at.%

Table 2. EDTS thickness and refractive index for A1-A3 samples.

Sample	EDTS thickness from SEM (µm)	EDTS thickness from prism coupler (µm)	SiO_2 thickness below EDTS layer from SEM (µm)	Refractive index
A1	0.806 ± 0.059	0.8336 ± 0.0541	0.561 ± 0.057	1.5587 ± 0.0004
A2	1.046 ± 0.021	0.9894 ± 0.0374	0.430 ± 0.017	1.5690 ± 0.0003
A3	1.562 ± 0.083	1.5593 ± 0.0371	0.222 ± 0.071	1.6172 ± 0.0005

The XRD spectra of all the samples, as shown in Fig. 2, showed that there were no sharp peaks, except at $2\theta = 70^{\circ}$, which were generated from the underlying crystalline silicon of SOS substrate [31], thus confirming the amorphous nature of the EDTS layer. The XRD pattern observed for sample A1 was similar to that of SOS. This similarity could be due to the fact that the Er-TZN content in A1 was lower than in those samples fabricated with higher laser energy. Such low concentrations were well dispersed in the silica matrix and therefore might not be detected by XRD. However, with increased laser energy, an additional feature was seen at around 30°, which indicated that the higher doping concentration in the silica changed the silica network from its original structure and made it look like that of a silicate glass [32].

Samples were also characterized to acquire the PL emission spectra. The PL around 1535 nm was produced by the transition $^4I_{13/2} \rightarrow {}^4I_{15/2}$ in Er^{3+} ions that were excited with a 980 nm laser diode at room temperature. The emission spectra for all samples are shown in Fig. 3. The spectral shape of all samples was very similar with peaks at the wavelengths of 1535 nm and 1543 nm. The appearance of the second peak was due to the Stark splitting effect [33]. PL intensity increased with an increasing laser energy (Table 3) due to an increase in Er^{3+} ions concentration. The measured typical full-width at half-maximum (FWHM) obtained from all the samples was 20 nm as shown in Table 3. The erbium emission spectra and FWHM obtained were also similar with those in other silicate hosts such as phosphosilicate, soda-lime silicate, and borosilicate glass [34,35]. This indicates that the Er-TZN had indeed permeated the silica network and formed silicate glass.

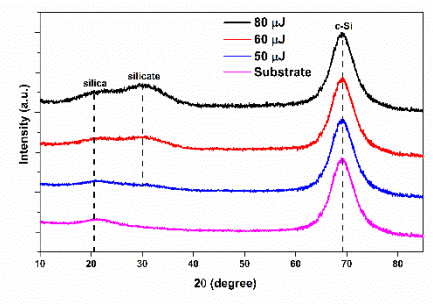

Fig. 2. XRD spectra of the samples fabricated with different fs-laser energies. The c-Si peak @ 70° was from the crystalline silicon of SOS substrate underneath EDTS and silica layer.

Table 3 shows that the PL lifetime variation with laser energy used. The PL lifetime decreased when the erbium concentration was increased. This was due to the increase in Er^{3+} ions in the EDTS, which in turn reduced the average spacing between Er-Er ions, thus increased the concentration quenching effect in which energy migration takes place due to energy transfer between Er^{3+} ions [35].

Additionally, we also analyzed the effect of the fs-laser repetition rate. Repetition rates used were 0.5 kHz and 1 kHz. XRD measurements showed that both EDTS layers were in the amorphous phase. The doped layer created with 0.5 kHz had an EDTS thickness of 0.412 µm or almost half the thickness of 1 kHz sample (0.806 µm) for the same deposition time. This variation was entirely expected, as the increase in layer thickness directly depended on the amount of ablated material and its subsequent interaction with silica. The doping concentration was much lower for the sample prepared at 0.5 kHz compared to the 1 kHz sample. The higher doping also resulted in a higher refractive index (n=1.5587) compared to n=1.5298 for the 0.5 kHz sample. As the sample prepared at 0.5 kHz had a lower erbium concentration, the PL lifetime measured was longer at 14.07 ms compared to the 1 kHz sample which had a PL lifetime of 12.29 ms. The FWHM of the PL

for both samples was almost equal sround 19-20 nm and matched the FWHM of other erbium doped silicate glasses.

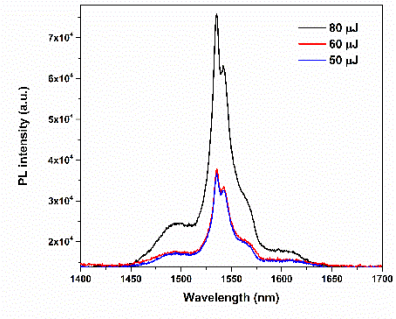

Fig. 3. Photoluminescence emission spectra around 1535 nm for samples prepared at different fs-laser energies. The excitation wavelength was 980 nm.

Table 3. FWHM and lifetime for EDTS samples obtained at different laser energies

Sample	FWHM (nm)	Photoluminescence lifetime (ms)
A1	20	12.29
A2	20	12.21
A3	20	10.79

In summary, we have demonstrated that by using the ULPD approach erbium doped tellurite glass containing zinc and sodium ions can be effectively doped into a SOS substrate to well beyond the usual solubility limit without detectable clustering. The highest erbium concentration we obtained is 0.53 at% (1.29×10^{20} cm^{-3}) (calculated based on silica glass density, 2.2 g/cm^{-3}) with an associated PL lifetime of 10.79 ms. Based on these values, the estimated optical gain by theoretical calculation is approximately 5 dB/cm, which could be improved by further increasing the Er doping concentration. This work also confirmed that the EDTS layer thickness, PL lifetime, erbium concentration and refractive index can be precisely controlled by adjusting the process parameters. Furthermore the thicknesses of these modified layers can be controlled to sub 100nm levels meaning that precise layering of such materials is also possible. Significantly, we have demonstrated the formation of high index contrast EDTS layers on a SOS substrate, which is suitable for integrated optical components.

Funding. EPRSC of the UK (project "SEAMATICS", EP/M015165/1).

Acknowledgment. The authors acknowledge financial support from Ministry of Education (MOE) of Malaysia and Universiti Teknologi MARA (UiTM) (Ph.D scholarship for Suraya Ahmad Kamil).

REFERENCES

1. X. Xia, J. Zou, T. Lang, and J. J. He, IEEE Photonics J. **4**, 2236 (2012).
2. Z. Jin and G. Peng, in *Progress in Electromagnetics Research Symposium 2005* (The Electromagnetics Academy, 2005), p. 58.
3. A. Politi, M. J. Cryan, J. G. Rarity, S. Yu, and J. L. O'Brien, Sci. **320**, 646 (2008).
4. J. Liu, M. Beals, J. Michel, and L. C. Kimerling, ECS Trans. **19**, 17 (2009).
5. V. Donzella, S. Faralli, and F. Di Pasquale, in 21st Annual Meeting of the IEEE Lasers and Electro-Optics Society (LEOS) (IEEE, 2008), p. 595.
6. J. L. Philipsen, C. L. Thomsen, L. Leick, Y. Shen, P. C. Nielsen, C. Laurent-Lund, M. G. Dyndgaard, and T. Feuchter, in *Proceedings of European Conference on Optical Communication* (AEI, 2003), p. 420.
7. A. J. Kenyon, Prog. Quantum Electron. **26**, 225 (2002).
8. K. Vu and S. Madden, Opt. Express **18**, 19192 (2010).
9. S. Sakida, T. Nanba and Y. Miura, Opt. Mat. **30**, 586 (2007).
10. V.A.G. Rivera, E.F. Chillcce, E. Rodriguez, C.L. Cesar, L.C. Barbosa, J. Non. Cryst. Solids **352**, 363 (2006).
11. F. Ren, Y.Z. Mei, C. Gao, L.G. Zhu and A. X. Lu, Trans. Nonferrous Met. Soc. China **22**, 2021 (2012).
12. F. Auzel and P. Goldner, Opt. Mater. **16**, 93 (2001).
13. N. D. Afify, G. Dalba, and F. Rocca, J. Phys. D Appl. Phys. **42**, 115416 (2009).
14. H. L. An, E. Y. B. Pun, H. D. Liu, and X. Z. Lin, Opt. Lett. **23**, 1197 (1998).
15. K. Bourhis, J. Massera, L. Petit, H. Ihalainen, A. Fargues, T. Cardinal, L. Hupa, M. Hupa, M. Dussauze, V. Rodriguez, C. Boussard-Plédel, B. Bureau, C. Roiland, and M. Ferraris, Mater. Res. Bull. **63**, 41 (2015).
16. P. G. Kik and A. Polman, MRS Bull. **23**, 48 (1998).
17. K. Hattori, T. Kitagawa, M. Oguma, H. Okazaki, and Y. Ohmori, J. Appl. Phys. g h**80**, 5301 (1996).
18. S. I. Seok, M. A. Lim, J. J. Ju, and M. H. Lee, J. Am. Ceram. Soc. **88**, 2380 (2005).
19. R. R. Gonçalves, G. Carturan, M. Montagna, M. Ferrari, L. Zampedri, S. Pelli, G. C. Righini, S. J. L. Ribeiro, and Y. Messaddeq, Opt. Mater. **25**, 131 (2004).
20. J. L. Ferrari, K. O. Lima, L. J. Q. Maia, and R. R. Gonçalves, Thin Solid Films **519**, 1319 (2010).
21. W. Huang, R. R. A. Syms, E. M. Yeatman, M. M. Ahmad, T. V. Clapp, and S. M. Ojha, IEEE Photonics Technol. Lett. **14**, 959 (2002).
22. G. C. Righini, S. Pelli, M. Ferrari, C. Armellini, L. Zampedri, C. Tosello, S. Ronchin, R. Rolli, E. Moser, M. Montagna, A. Chiasera, and S. J. L. Ribeiro, Opt. Quantum Electron. **34**, 1151 (2002).
23. C. E. Chryssou and C. W. Pitt, IEEE J. Quantum Electron. **34**, 282 (1998).
24. K. Hattori, T. Kitagawa, M. Oguma, Y. Ohmori, and M. Horiguchi, Electron. Lett. **30**, 856 (1994).
25. L. H. Sloof, M. J. A. de Dood, A. van Blaaderen, and A. Polman, J. Non. Cryst. Solids **296**, 158 (2001).
26. S. M. Cho, Y. T. Kim, D. H. Yoon, Y. M. Im, and G. E. Jang, J. Korean Phys. Soc. **42**, S947 (2003).
27. M. W. Sckerl, S. A. Guldberg-Kjær, C. Laurent-Lund, and M. R. Poulsen, in *25th European Conference on Optical Communication* (Société des électriciens et des électroniciens, 1999), p. 48.
28. J. Chandrappan, M. Murray, T. Kakkar, P. Petrik, E. Agocs, Z. Zolnai, D. P. Steenson, A. Jha, and G. Jose, Sci. Rep. **5**, 14037 (2015).
29. J. Chandrappan, M. Murray, P. Petrik, E. Agocs, Z. Zolnai, A. Tempez, S. Legendre, D. P. Steenson, A. Jha, and G. Jose, Opt. Mater. Express **5**, 2849 (2015).
30. M. N. Azlan, M. K. Halimah, S. Z. Shafinas, and W. M. Daud, Mater. Express **5**, 211 (2015).
31. G. G. Pethuraja, R. E. Welser, A. K. Sood, C. Lee, N. J. Alexander, H. Efstathiadis, P. Haldar, and J. L. Harvey, Mater. Sci. Appl. **03**, 67 (2012).
32. H. Zhang, J. H. Zhou, Q. L. Zhang, and H. Yang, J. Inorg. Mater. **28**, 785 (2013).
33. A. Polman, Phys. B **300**, 78 (2001).
34. A. Polman, Appl. Phys. Rev. **82**, 1 (1997).
35. E. Snoeks, P. G. Kik, and A. Polman, Opt. Mater. **5**, 159 (1996).

REFERENCES

1. X. Xia, J. Zou, T. Lang, and J. J. He, "Experimental demonstration of birefringence compensation using angled star couplers in silica-based arrayed waveguide grating," IEEE Photonics J. **4**, 2236 (2012).

2. Z. Jin and G. Peng, "Desiging optical switches based on silica multimode interference devices," in *Progress in Electromagnetics Research Symposium 2005* (The Electromagnetics Academy, 2005), p. 58.
3. A. Politi, M. J. Cryan, J. G. Rarity, S. Yu, and J. L. O'Brien, "Silica-on-silicon waveguide quantum circuits," Sci. **320**, 646 (2008).
4. J. Liu, M. Beals, J. Michel, and L. C. Kimerling, "Light up the future of silicon microprocessors," ECS Trans. **19**, 17 (2009).
5. V. Donzella, S. Faralli, and F. Di Pasquale, "Effect of Si-nc to Er^{3+} coupling ratio and multimode resonant pumping on EDWAs performance," in 21st Annual Meeting of the IEEE Lasers and Electro-Optics Society (LEOS) (IEEE, 2008), p. 595.
6. J. L. Philipsen, C. L. Thomsen, L. Leick, Y. Shen, P. C. Nielsen, C. Laurent-Lund, M. G. Dyndgaard, and T. Feuchter, "Erbium-doped waveguide amplifier (EDWA) technology and components," in *Proceedings of European Conference on Optical Communication* (AEI, 2003), p. 420.
7. A. J. Kenyon, "Recent developments in rare-earth doped materials for optoelectronics," Prog. Quantum Electron. **26**, 225 (2002).
8. K. Vu and S. Madden, "Tellurium dioxide erbium doped planar rib waveguide amplifiers with net gain and 2.8dB/cm internal gain," Opt. Express **18**, 19192 (2010).
9. S. Sakida, T. Nanba and Y. Miura, "Optical properties of Er^{3+}-doped tungsten tellurite glass waveguides by Ag^{+}-Na^{+} ion exchange," Opt. Mat. **30**, 586 (2007).
10. V.A.G. Rivera, E.F. Chillcce, E. Rodriguez, C.L. Cesar, L.C. Barbosa, "Planar waveguides by ion exchange in Er^{3+}-doped tellurite glass," J. Non. Cryst. Solids **352**, 363 (2006).
11. F. Ren, Y.Z. Mei, C. Gao, L.G. Zhu and A. X. Lu, "Themal stability and judd-ofelt analysis of optical properties of Er^{3+}-doped tellurite glass," Trans. Nonferrous Met. Soc. China **22**, 2021 (2012).
12. F. Auzel and P. Goldner, "Towards rare-earth clustering control in doped glasses," Opt. Mater. **16**, 93 (2001).
13. N. D. Afify, G. Dalba, and F. Rocca, "XRD and EXAFS studies on the structure of Er^{3+}-doped SiO_2–HfO_2 glass-ceramic waveguides: Er^{3+}-activated HfO_2 nanocrystals," J. Phys. D Appl. Phys. **42**, 115416 (2009).
14. H. L. An, E. Y. B. Pun, H. D. Liu, and X. Z. Lin, "Effects of ion clusters on the performance of a heavily doped erbium-doped fiber laser," Opt. Lett. **23**, 1197 (1998).
15. K. Bourhis, J. Massera, L. Petit, H. Ihalainen, A. Fargues, T. Cardinal, L. Hupa, M. Hupa, M. Dussauze, V. Rodriguez, C. Boussard-Plédel, B. Bureau, C. Roiland, and M. Ferraris, "Influence of P_2O_5 and Al_2O_3 content on the structure of erbium-doped borosilicate glasses and on their physical, thermal, optical and luminescence properties," Mater. Res. Bull. **63**, 41 (2015).
16. P. G. Kik and A. Polman, "Erbium-doped optical-waveguide amplifiers on silicon," MRS Bull. **23**, 48 (1998).
17. K. Hattori, T. Kitagawa, M. Oguma, H. Okazaki, and Y. Ohmori, "Optical amplification in Er^{3+}-doped P_2O_5–SiO_2 planar waveguides," J. Appl. Phys. **80**, 5301 (1996).
18. S. I. Seok, M. A. Lim, J. J. Ju, and M. H. Lee, "Optical properties of Er-doped Al_2O_3-SiO_2 films prepared by a modified sol–gel process," J. Am. Ceram. Soc. **88**, 2380 (2005).
19. R. R. Gonçalves, G. Carturan, M. Montagna, M. Ferrari, L. Zampedri, S. Pelli, G. C. Righini, S. J. L. Ribeiro, and Y. Messaddeq, "Erbium-activated HfO_2-based waveguides for photonics, " Opt. Mater. **25**, 131 (2004).
20. J. L. Ferrari, K. O. Lima, L. J. Q. Maia, and R. R. Gonçalves, "Sol-gel preparation of near-infrared broadband emiting Er^{3+}-doped SiO_2-Ta_2O_5 nanocomposites films," Thin Solid Films **519**, 1319 (2010).
21. W. Huang, R. R. A. Syms, E. M. Yeatman, M. M. Ahmad, T. V. Clapp, and S. M. Ojha, " Fiber-device-fiber gain from a sol-gel erbium-doped waveguide amplifier," IEEE Photonics Technol. Lett. **14**, 959 (2002).
22. G. C. Righini, S. Pelli, M. Ferrari, C. Armellini, L. Zampedri, C. Tosello, S. Ronchin, R. Rolli, E. Moser, M. Montagna, A. Chiasera, and S. J. L. Ribeiro, " Er-doped silica-based waveguides prepared by different techniques: RF-sputtering, sol-gel and ion-exchange," Opt. Quantum Electron. **34**, 1151 (2002).
23. C. E. Chryssou and C. W. Pitt, "Er^{3+}-doped Al_2O_3 thin films by plasma-enhanced chemical vapor deposition (PECVD) exhibiting a 55-nm optical bandwidth," IEEE J. Quantum Electron. **34**, 282 (1998).
24. K. Hattori, T. Kitagawa, M. Oguma, Y. Ohmori, and M. Horiguchi, "Erbium-doped silica-based waveguide amplifier integrated with a 980/1530 nm WDM coupler," Electron. Lett. **30**, 856 (1994).
25. L. H. Sloof, M. J. A. de Dood, A. van Blaaderen, and A. Polman, "Effects of heat treatment and concentration on the luminescence properties of erbium-doped silica sol-gel films," J. Non. Cryst. Solids **296**, 158 (2001).
26. S. M. Cho, Y. T. Kim, D. H. Yoon, Y. M. Im, and G. E. Jang, "Optical characterization of silica based waveguide prepared by plasma enhanced chemical vapor deposition,"J. Korean Phys. Soc. **42**, S947 (2003).
27. M. W. Sckerl, S. A. Guldberg-Kjær, C. Laurent-Lund, and M. R. Poulsen, "Loss-less planar waveguide 1:4 power splitter at 1550 nm," in *25th European Conference on Optical Communication* (Société des électriciens et des électroniciens, 1999), p. 48.
28. J. Chandrappan, M. Murray, T. Kakkar, P. Petrik, E. Agocs, Z. Zolnai, D. P. Steenson, A. Jha, and G. Jose, "Target dependent femtosecond laser plasma implantation dynamics in enabling silica for high density erbium doping," Sci. Rep. **5**, 14037 (2015).
29. J. Chandrappan, M. Murray, P. Petrik, E. Agocs, Z. Zolnai, A. Tempez, S. Legendre, D. P. Steenson, A. Jha, and G. Jose, " Doping silica beyond limits with laser plasma for active photonic materials," Opt. Mater. Express **5**, 2849 (2015).
30. M. N. Azlan, M. K. Halimah, S. Z. Shafinas, and W. M. Daud, "Electronic polarizability of zinc borotellurite glass system containing erbium nanoparticles," Mater. Express **5**, 211 (2015).
31. G. G. Pethuraja, R. E. Welser, A. K. Sood, C. Lee, N. J. Alexander, H. Efstathiadis, P. Haldar, and J. L. Harvey, "Effect of Ge incorporation on bandgap and photosensitivity of amorphous SiGe thin films," Mater. Sci. Appl. **03**, 67 (2012).
32. H. Zhang, J. H. Zhou, Q. L. Zhang, and H. Yang, "Mechanical and optical properties of ion-exchange strengthened glass coated with sol-gel derived ZrO_2-SiO_2 Film," J. Inorg. Mater. **28**, 785 (2013).
33. A. Polman, "Erbium as a probe of everything?," Phys. B **300**, 78 (2001).
34. A. Polman, "Erbium implanted thin film photonic materials," Appl. Phys. Rev. **82**, 1 (1997).
35. E. Snoeks, P. G. Kik, and A. Polman, "Concentration quenching in erbium implanted alkali silicate glasses," Opt. Mater. 5, 159 (1996).